IOP Conf. Series: Materials Science and Engineering **140** (2016) 012011 doi:10.1088/1757-899X/140/1/012011

Numerical and experimental study of electron-beam coatings with modifying particles FeB and FeTi

Olga Kryukova, Kseniya Kolesnikova, Nina Gal'chenko

Institute of Strength Physics and Materials Science SB RAS, Tomsk, Russia

E-mail: okruk@ispms.tsc.ru

Abstract. An experimental study of wear-resistant composite coatings based on titanium borides synthesized in the process of electron-beam welding of components thermo-reacting powders are composed of boron-containing mixture. A model of the process of electron beam coating with modifying particles of boron and titanium based on physical-chemical transformations is supposed. The dissolution process is described on the basis of formal kinetic approach. The result of numerical solution is the phase and chemical composition of the coating under nonequilibrium conditions, which is one of the important characteristics of the coating forming during electron beam processing. Qualitative agreement numerical calculations with experimental data was shown.

1. Introduction

Powder metallurgy methods combined with using of concentrated energy fluxes have special capabilities for obtaining materials and compositions with given (improved) properties.

The wear resistant composite coatings on the basis of titanium borides, which are synthesized from thermoreactive powder components of a boron-containing mixture at electron beam surfacing, are interesting for applications today.

It is known that in electron beam surfacing of thermoreactive powders an additional amount of heat is released in the fusion zone due to the exothermal reaction between the mixture components. This allows, with the same electron beam power, the deposition of coatings with a required content of the fine-grained refractory component. The physico-mechanical properties of the coatings can vary in a wide range depending on the proportion and sizes of initial components in the fused mixture. The coating structure formation ends with the convective mixing of solid-liquid melts, which have formed after the complete dissolution of components having different viscosity because of different chemical composition and different content of refractory particles in them [1,2].

The degree of the melt mixing depends on many factors, including the size of initial components. Obviously, changes in the granulometric composition of the fused powder would greatly affect the crystallization rate and completeness of phase transformations at electron beam surfacing, thus defining the microstructure, phase composition and service properties of deposited coating.

The aim of the paper is to study the simultaneous synthesis of boride compounds and formation of composite coatings on their basis under vacuum electron-beam treatment of thermoreactive powders.

2. Materials and experimental procedure

The mixture for the electron beam surfacing of coatings and their further examination was prepared of low-cost thermoreactive ferroalloy powders FeB (grade FB-20) and FeTi (grade FTi65) widely used in steel and alloy metallurgy.

Table 1. Chemical composition of ferroalloys (wt %) used in the study.

Grade	B	Si	Al	C	S	P	Cu	Ti	V
FB-20	20	2	3	0.05	0.01	0.02	0.05	–	–
FTi65	–	1	5	0.4	0.05	0.05	04	65	3

The composite material with a definite proportion of the refractory compound (titanium diboride) and metal binder (iron) was produced by the chemical reaction $xFeB + yFeTi \rightarrow TiB_2 + Fe + Q$.
The mixture composition was calculated so that to produce the TiB_2-Fe composite coating with 33 mass % of titanium diboride. The given percentage is provided by the proportion of the used mixture components FeB – FeTi = 1:1.
To study the features of the phase and structure formation in the fused layer, three variants of FeB – FeTi powder mixtures were electron-beam deposited in experiments. The mixtures differed in the granulometric composition of initial components: 1) FeB(50–125 μm)+FeTi(200–315 μm); 2) FeB(200–315 μm)+FeTi(200–315 μm); 3) FeB(200–315 μm) + FeTi(50–200 μm).
The coatings were electron-beam deposited on steel substrates (grade St.3) in 2–4 passes at accelerating voltage 28 kV. The beam diameter was 1.0 mm, scanning length 12 mm, and substrate velocity 2 mm/s. The fused layer thickness was 2–3 mm.
The phase composition was X-ray examined by a diffractometer DRON-4, the chemical composition was studied by a setup KAMEBAX-MIKROBEAM for X-ray spectrum microanalysis on an area of 1 μm. The coating microstructure was examined by a light microscope MIM-9. The microhardness $H\mu$ was measured by a device PMT-3 under the load P = 50 g.

3. Experimental results and discussion

3.1. Coatings of thermoactive powder mixture FeB(50–125 μm)+FeTi(200–315 μm) (coating 1)
The comparative analysis has shown that the given coating has the most heterogeneous structure across the thickness. Fragments of the structure are depicted in Figure 1. The structure is typically observed after the crystallization of melts of nonuniform concentration. The uneven microhardness distribution across the coating thickness clearly demonstrates its heterogeneity (Figure 4a).

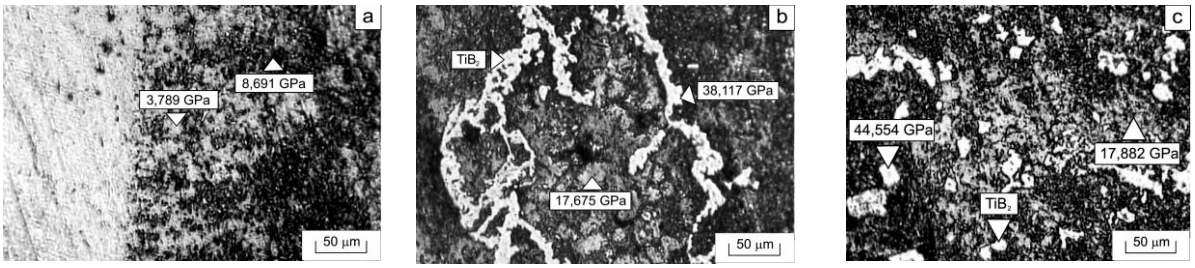

Figure 1. Microstructure of the coating produced of thermoreactive powder mixture FeB(50–125 μm) + FeTi(200–315 μm): *a* — interface with the substrate; *b* — middle of the deposited layer; *c* — subsurface coating area.

The performed investigation suggests the following mechanism of structure formation at surfacing. First, FeTi particles of size 200–315 μm melt (T_m = 1200°C) and form a ferrotitanium melt. When contacting with a conglomerate of FeB particles (T_m = 1540°C), the melt forms a ring structure around the FeB particles due to the formation of low-temperature contact eutectics. The ring structure consists of titanium diboride crystals of hardness H = 38 GPa (Figure 1b). The formation of the liquid phase — ferrotitanium melt — favors further refinement of the FeB particles that rapidly dissolve in the FeTi

melt and saturate it with boron. The final coating structure is a result of the solidification of the two heterogeneous melts.

Since the electron beam surfacing is carried out in many passes, the deposition of next layers increases the substrate temperature, lifetime of the liquid metal bath formed on the surface of the underlying deposited layer and reduces the melt crystallization rate. After the crystallization the matrix structure of the composite coating is an alloyed solid solution with highly nonuniform concentration, fine and coarse iron and titanium borides as well as with numerous nonequilibrium boride-based eutectics. This structure leads to the formation of heterogeneous coatings.

Figure 1,c illustrates the microstructure of the FeB(50–125 μm)+FeTi(200–315 μm) coating surface with solitary titanium diboride crystals, which evidently entered the melt due to convective mass transfer from the underlying layer in the middle of the coating. There is a structure on the coating surface which consists of large titanium diboride crystals (7÷22 μm) and heterogeneous metal binder with nonuniform hardness. The binder is chaotically hardened by fine-grained (≤1 μm) compounds of titanium borides of other stoichiometry (Figure 1,c). This is confirmed by the data of X-ray phase analysis showing that, along with pronounced reflections from TiB_2 and α-Fe, phases TiB, Ti_2B and Ti_2B_5 are registered.

3.2. Coatings of thermoreactive powder mixture FeB(200–315 μm)+FeTi(200–315 μm) (coating 2)

The microstructural analysis of coatings produced of a mixture of coarse-grained powders having the same granulometric composition (coating *2*) has also shown that the coating structure is heterogeneous across the thickness (Figure 2).

This is probably due to the fact that, because of the large powder particles and high crystallization rate, the time period when the concentration of alloying elements in the formed melt becomes uniform was too short. The nonuniform melt crystallization resulted in the formation of specific structures at the interface with the substrate and in the middle of the deposited layer. The structures have irregularly shaped regions in the form of light unetched globules whose chemical composition differs across the coating thickness. By the data of X-ray spectrum microanalysis, the above solid solution regions at the interface have the composition of Fe_2B and hardness $H \approx 14$ GPa (Figure 2,a). In the middle of the coating (Figure 2,c) the globules became three-dimensional and darker in color. These regions have the composition of FeB and hardness H = 16–18 GPa. The FeB formation is evidently caused by the fact that with distance from the coating – substrate interface and increasing number of passes the melt temperature grows and the degree of its saturation with boron also increases owing to a more complete dissolution of initial FeB powder particles.

Such melt crystallizes with the formation of regions in the coating structure which have the composition of FeB, being separated by fine-grained particles and their conglomerates whose hardness (H = 32.5 GPa) corresponds to the TiB_2 phase. One can also see from Figure 2,b,c that the metal binder structure between the unetched regions exhibits heterogeneous phase morphology and nonuniform hardness (H = 6–19 GPa). It has numerous regions with dendritic and eutectic structure whose hardness reduces with the eutectic size refinement. According to the X-ray phase analysis, the eutectics can be the Fe_2B-Fe and TiB_2-Fe compounds [3].

When surfacing powders of the given granulometric composition, we observed the highest fluidity of the formed melt as compared to coatings *1* and *3*.

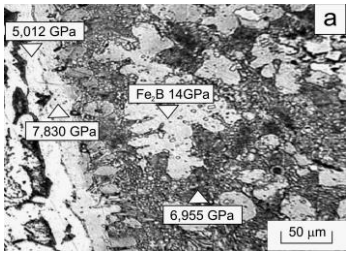

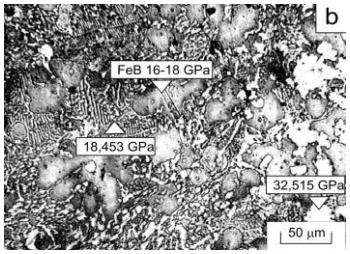

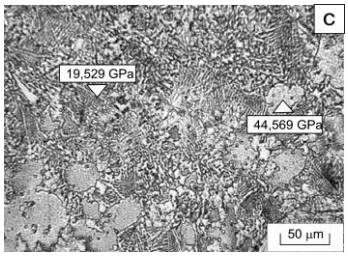

Figure 2. Microstructure of the coating produced of thermoreactive powder mixture FeB(200–315 μm)+FeTi(200–315 μm): *a*) interface with the substrate; *b*) middle of the deposited layer; *c*) subsurface coating zone.

3.3. Coatings of thermoreactive powder mixture FeB(200–315 μm)+FeTi(50–200 μm) (coating 3)
After coating deposition we had a layered structure, in which every layer mainly contained one phase component across its thickness (Figures. 3, a–c).

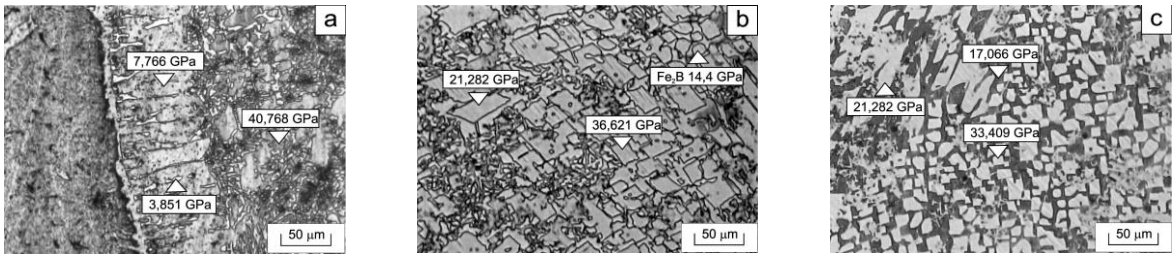

Figure 3. Microstructure of the coating produced of thermoreactive powder mixture FeB(200–315 μm)+FeTi(50–200 μm): *a*) interface with the substrate; *b*) middle of the deposited layer; *c*) subsurface coating region.

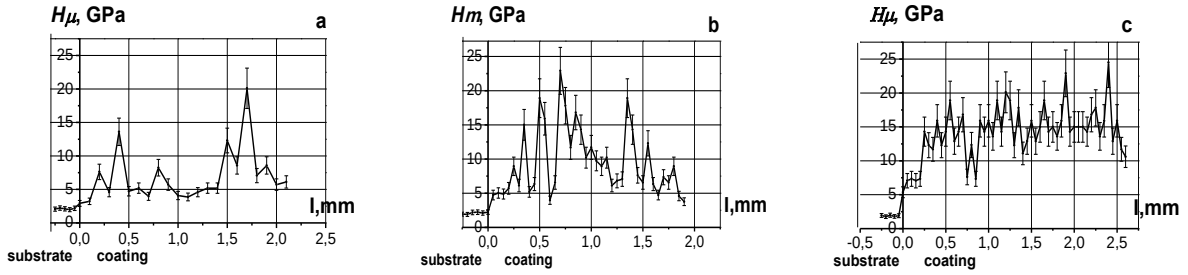

Figure 4. Distribution of microhardness *H*μ in the coating: *a*) FeB(50–125 μm) + FeTi(200–315 μm); *b)* FeB(200–315 μm)+FeTi(200–315 μm); *c*) FeB(200–315 μm)+FeTi(50–200 μm).

In the middle of the coating at 1.3 mm from the interface with the substrate (Figure 3, b) the structure mainly consists of rounded Fe_2B particles of size 8–12 μm and hardness H = 14.4 GPa, rectangular titanium diboride crystals (4–6 μm) and larger elongated titanium boride particles embedded in the Fe_2B-Fe eutectic matrix. The subsurface coating region (Figure 3, c) also has heterogeneous phase composition: the left part of the microscan demonstrates aggregates of titanium borides, the right part — a microstructure region with uniform distribution of 10–17 μm light crystals in the metal binder which are titanium borides and diborides (TiB, TiB_2). The hardness of the particles is in the interval H = 22–34 GPa.

4. Mathematical problem formulation

The mathematical formulation about the phase formation and chemical structure of the coating of the low-carbon steel substrate during electron beam surfacing with modifying particles boron and titanium includes heat equation [4-6]

$$c\rho\frac{\partial T}{\partial t}=\frac{\partial}{\partial x}\left(\lambda\frac{\partial T}{\partial x}\right)+\frac{\partial}{\partial y}\left(\lambda\frac{\partial T}{\partial y}\right)+\sum Q_{ch,i}\varphi_i+\sum_{j=B,Ti}Q_{p,j}\Phi_j(T,\eta_{p,j})-\frac{(\varepsilon\sigma T^4-q_e)}{h} \qquad (1)$$

and the equation for the particles, which take into account the delivery of the particles in treatment area, turbulent mixing of the particles in the melt under pressure exerted by moving source and dissolution

$$\frac{\partial \eta_{p,j}}{\partial t} = q_{m,j} - \Phi_j(T, \eta_{p,j}) + D_{eff}\left(\frac{\partial^2 \eta_{p,j}}{\partial x^2} + \frac{\partial^2 \eta_{p,j}}{\partial y^2}\right), \quad j = B, Ti \tag{2}$$

where D_{eff} is average mixing ratio of the particles in the melt $D_{eff} = D_T$, $T \geq T_{ph}$; $D_{eff} = D_S$, $T < T_{ph}$; $D_S << D_T$.

The external source moves along the plate surface at the velocity V, and the energy therein is distributed according to the law

$$q_e = \begin{cases} 0 & , y > h_0; \\ q_0 \exp\left(-(x^2 - Vt)/a_t^2\right) & , y \leq h_0, \end{cases} \tag{3}$$

where q_0 is the maximum density of the heat flux; a_t is the effective radius of the source; the parameter h_0 is proportional to the scanning width.

The particle flux density is distributed according to a Gaussian

$$q_{m,j} = q_{m0,j} \exp\left[-\left((x - x_a - Vt)^2 + y^2\right)/a_p^2\right] \tag{4}$$

where q_0 is the maximum density of the heat flux; a_t is the effective radius of the source; the parameter h_0 is proportional to the scanning width.

The rate of dissolution obeys the law $\Phi_j(T, \eta_p) = \varphi_{p,j}(\eta_{p,j}) k_{Sol} \exp\left(-E_{Sol,j}/RT\right)$, where value of activation energy E_{Sol} is determined by features of the dissolution process for particles of a given type. . View of kinetic function depends on the processes that determine the dissolution rate at the micro level. Constant k_{Sol} is determined by the characteristics of the local hydrodynamic flow in the vicinity of the particle trapped in the melt [7].

n the volume of the material the chemical reactions proceed with the total heat release (taking in the heat equation) $Q_{ch} = \rho \sum_{k=1}^{n} h_k \cdot (dC_k/dt)$ where h_k – partial enthalpy (formation) k-th substance, ρ – the material density of the base, C_k – mass concentrations of individual substances and compounds in the mixture, n – number of substances involved in the reactions.

Mass concentrations are related to the molar concentration ratios:

$$C_k = \frac{\rho_k}{\rho}, \text{ since } y_k = \frac{\rho_k}{M_k}, \text{ then } C_k = \frac{y_k M_k}{\sum_{i=1}^{n} y_i M_i + y_{Ti} M_{Ti} + y_B M_B}.$$

Molar concentration we find from solutions of the kinetic problem.

In accordance with the phase diagram of the Fe-B-Ti system we can write a system of chemical reactions:

1). $Fe + B \rightarrow FeB$
2). $Fe + Ti \rightarrow FeTi$
3). $Ti + 2B \rightarrow TiB_2$
4). $Ti + B \rightarrow TiB$
5). $2Fe + B \rightarrow Fe_2B$
6). $2Fe + B \rightarrow TiFe_2$

We introduce the notations for the molar concentrations of the reactants and reaction products involved in the conversion of $y_1 = [\mathrm{Fe}]$; $y_2 = [\mathrm{B}]$; $y_3 = [\mathrm{Ti}]$; $y_4 = [\mathrm{FeB}]$; $y_5 = [\mathrm{FeTi}]$; $y_6 = [\mathrm{TiB_2}]$; $y_7 = [\mathrm{TiB}]$; $y_8 = [\mathrm{Fe_2B}]$; $y_9 = [\mathrm{TiFe_2}]$ mol/m^3. Then, for each substance we can concretize equation. For example, for the titanium and boron we have

$$\frac{dy_2}{dt} = \frac{\rho_B}{M_B}\Phi_B - (\varphi_1 + 2\varphi_3 + \varphi_4 + \varphi_5 + \varphi_6 + 4\varphi_7), \qquad \frac{dy_3}{dt} = \frac{\rho_{Ti}}{M_{Ti}}\Phi_{Ti} - (\varphi_2 + \varphi_3 + \varphi_4 + 3\varphi_7).$$

The rate of each reaction depends on the concentration in accordance with the law of mass action, and the rate depends on the temperature in accordance with the Arrhenius law: $\varphi_i = k_{0i}\exp(-E_{ai}/RT)y^{m_i}y^{n_i}$, where i –number of reaction. For many of the written out reactions the experimental data about the formal kinetic parameters are missing. The reaction rates constants k_{0i}, activation energy E_{ai} and heats of reactions Q_i is determined using known thermodynamic formulas [8].

Generally, heat capacity in (1) is complex function of temperature and composition. Near the melting temperature the heat capacity increases rapidly, it represents formula

$$(c\rho)_{eff} = c\rho + L_{ph}\rho_{b\_s}(1-\eta_p)\delta(T - T_{ph}) \tag{5}$$

where δ – the Dirac delta function, L_{ph} – latent heat of melting, T_{ph} – melting point of pure "material of basis"; index "b" corresponds to the material of the base; "s" – the solid phase; "p" – particles.

$$c\rho = (c\rho)_S(1-\eta_{p\_B}-\eta_{p\_Ti}) + (c\rho)_B\eta_{p-B} + (c\rho)_{Ti}\eta_{p-Ti}, \tag{6}$$

$$(c\rho)_S = (c\rho)_{Fe}\xi_{Fe} + (c\rho)_B\xi_B + (c\rho)_{Ti}\xi_{Ti} + \sum_{k=1}^{n}(c\rho)_k\xi_k,$$

ξ_k is the fraction of newly formed chemical compounds $\xi_k = y_k/(\sum_{i=1}^{n} y_i + y_{Fe} + y_B + y_{Ti})$.

Boundary conditions reflect a lack of heat source at an infinite distance from molten pool and on the end of the plate, adopted as the starting point.

At the initial time we have the conditions

$$t = 0: \quad T = T_0, \qquad \eta_{p,j} = 0, \qquad \eta_{Fe} = 1, \qquad y_{Fe} = 0.141. \tag{7}$$

5. Analysis of results

Analysis of the results of the numerical analysis of the problem shows that as the source moves along treated surface quasistationary regime establishes [4, 9]. The power density of the heat source and the flux density of the particles influence on the shape and size of the molten pool and heat affected zone, for steady-state, also (Figure 5). The molten pool is painted dark gray color. The heat affected zone width corresponds to maximum size of light gray color area along y axis defined by temperature $T = 900\,K$.

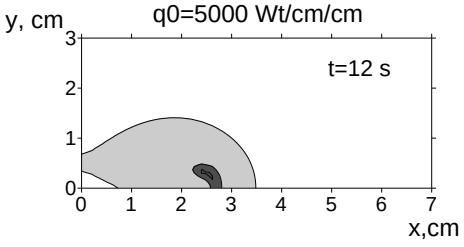

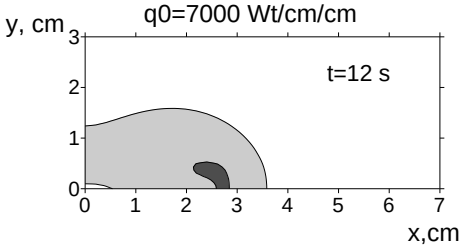

Figure 5. Influence of source power density on shape and size of molten pool and heat affected zone at the moment of steady state quasi-stationary regime. $q_{m0,B} = 0.7$ 1/s; $q_{m0,Ti} = 2.1$ 1/s .

Heterogeneous character the molten pool is connected with chemical reactions and mixing. The concentration distributions $C_i(x,0)$ at different times t and for different values q_0 of power density source are shown in Figure 6. Obviously, the higher source power density, the larger number of particles dissolving in the molten pool. Figure 6b allows estimate composition of formed surface layer.

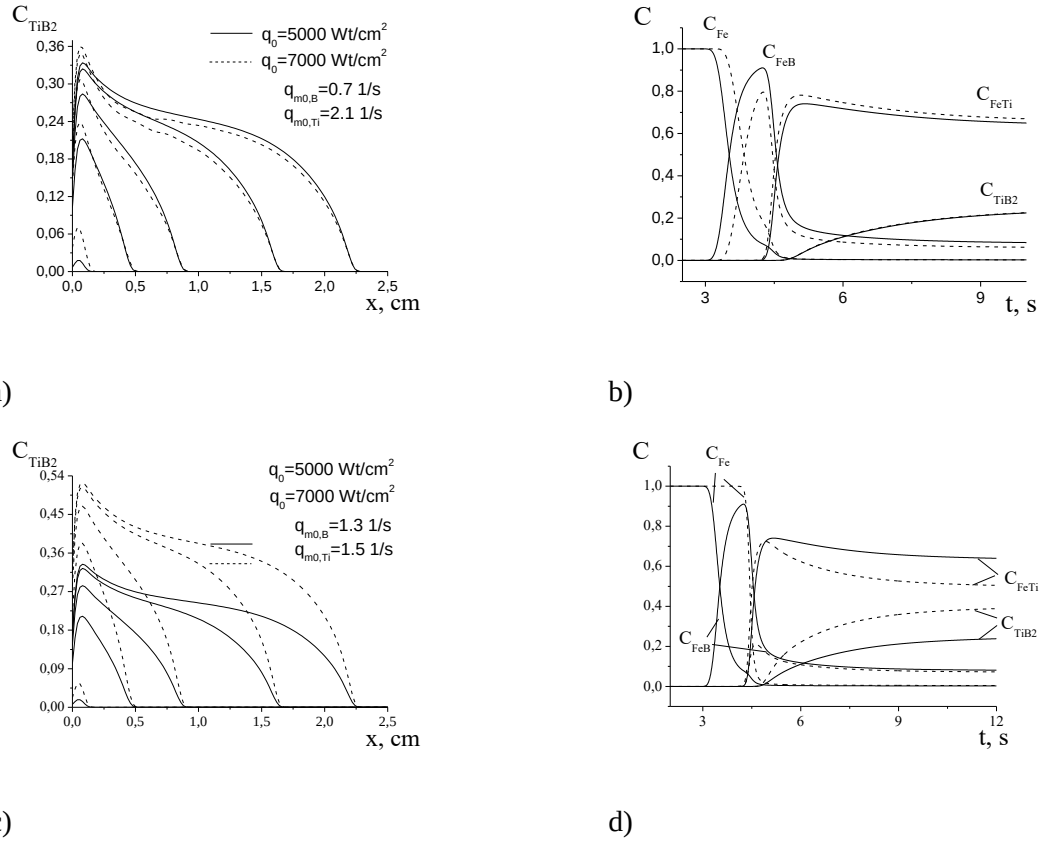

Figure 6. a), c) The distribution of the relative TiB_2 mass concentration along Ox axis at various times *t*; b), d) dependence of the relative mass concentrations of iron and forming compounds over time for different density of the particle flux. $V = 0.2$ cm/s.

6. Conclusion

1. The electron beam surfacing of thermoreactive Fe-B-Ti powders allows producing composite coatings on the basis of refractory titanium borides synthesized under the electron beam in vacuum. Such coatings exhibit high abrasive wear resistance and low wear rate in dry friction.
2. The granulometric composition of the fused powder mixtures strongly influences the physico-chemical processes occurring in the molten bath under the electron beam. It defines the coating properties that depend on the structure, proportion of boride phases and the metal binder, and the degree of solid solution hardening.
3. The model of the technological process of electron beam treatment of the material surface with modifying particles titanium and boron with accounting of formation of chemical compounds is supposed. All formal kinetic parameters included in the model are estimated. It is shown that the phase

and chemical composition of formed coating strongly depends on both the relations of components (fraction of particles) and the parameters characterizing the rate of heating (rate of movement of the source, flow density of energy and particles). The dependence of the coating composition on the beam power density and the density of the particle flux is illustrated. Similar dependence was observed in the experimental investigations performed on real systems [3, 10].

Acknowledgments

The work was carried out in the framework of the Fundamental Research Program of the State Academies of Sciences for 2013–2020. Project 23.2.1.

References

[1] Paton B E 1973 *Electron beam coating and refining of metals and* alloys (Kiev: Naukova Dumka)
[2] Galchenko N K, Belyuk S I, Panin V E *et al* 2002 *Fiz. Khim. Obrab. Materialov* **4** 68
[3] Kolesnikova K A, Galchenko N K 2006 *Physical Mesomechanics* 9 165–168
[4] Kryukova O N, Knyazeva A G 2006 *Physical Mesomechanics* 9 65–68
[5] Knyazeva A G, Pobol I L, Gordienko A I, Demidov V N, Kryukova O N, Oleschuk I G 2007 *Physical Mesomechanics* 10 **3-4** 207–220
[6] Kryukova O N 2006 *Bulletin TPU* **6** 120 (in Russian)
[7] Frolov V F 1998 *Theoretical Foundations of Chemical Engineering* 32 **4** 398
[8] Kryukova O N, Knyazeva A G 2014 *Russian Physics Journal* 57 **9/3** 113 (in Russian).
[9] Kryukova O N, Knyazeva A G 2007 *Journal of Applied Mechanics and Technical Physics* 48 **1** 109–118
[10] Galchenko N K, Belyuk S I, Kolesnikova K A, Galchenko V G 2010 *Deformation and fracture of materials* **4** 25